THE JOURNAL OF BIOLOGICAL CHEMISTRY VOL. 283, NO. 42, pp. 28767–28776, October 17, 2008

On the Mechanism of Quinol Oxidation at the Q_P Site in the Cytochrome bc_1 Complex

*STUDIED USING MUTANTS LACKING CYTOCHROME b_L OR b_H**

Received for publication, April 18, 2008, and in revised form, August 15, 2008 Published, JBC Papers in Press, August 18, 2008, DOI 10.1074/jbc.M803013200

Shaoqing Yang, He-Wen Ma, Linda Yu, and Chang-An Yu[1]

From the Department of Biochemistry and Molecular Biology, Oklahoma State University, Stillwater, Oklahoma 74078

To elucidate the mechanism of bifurcated oxidation of quinol in the cytochrome bc_1 complex, *Rhodobacter sphaeroides* mutants, H198N and H111N, lacking heme b_L and heme b_H, respectively, were constructed and characterized. Purified mutant complexes have the same subunit composition as that of the wild-type complex, but have only 9–11% of the electron transfer activity, which is sensitive to stigmatellin or myxothiazol. The E_m values for hemes b_L and b_H in the H111N and H198N complexes are −95 and −35 mV, respectively. The pseudo first-order reduction rate constants for hemes b_L and b_H in H111N and H198N, by ubiquiniol, are 16.3 and 12.4 s^{-1}, respectively. These indicate that the Q_p site in the H111N mutant complex is similar to that in the wild-type complex. Pre-steady state reduction rates of heme c_1 by these two mutant complexes decrease to a similar extent of their activity, suggesting that the decrease in electron transfer activity is due to impairment of movement of the head domain of reduced iron-sulfur protein, caused by disruption of electron transfer from heme b_L to heme b_H. Both mutant complexes produce as much superoxide as does antimycin A-treated wild-type complex. Ascorbate eliminates all superoxide generating activity in the intact or antimycin inhibited wild-type or mutant complexes.

The cytochrome bc_1 complex, also known as complex III or ubiquinol-cytochrome *c* oxidoreductase, is an essential segment of the electron transfer chain in mitochondria and photosynthetic bacteria (1). The complex catalyzes electron transfer from quinol to cytochrome *c* (c_2 in some bacteria) with concomitant translocation of protons across the inner membrane of mitochondria or cytoplasmic membrane of bacteria. Intensive biochemical and biophysical studies on this complex (2–4) have led to the formulation of the "protonmotive Q-cycle" mechanism for electron and proton transfer in this complex (5–7). The key step of the Q-cycle mechanism is the bifurcated oxidation of quinol at the quinol oxidation site (Q_P). In the Q-cycle mechanism, it was postulated that the first electron of quinol is transferred to the "high potential chain," consisting of iron-sulfur protein (ISP)[2] and cytochrome c_1. Then the second electron of quinol, via a transient semiquinone, is passed through the "low potential chain" consisting of cytochromes b_L and b_H, to reduce ubiquinone or ubisemiquinone bound at the quinol reduction site (Q_N). One drawback of this sequential scheme is the lack of a "functional" semiquinone at the Q_P site (8–10), even though some radicals have been reported under abnormal conditions (11, 12). Recently, pre-steady state kinetic analysis of the reduction of cytochrome b_L and ISP in a same sample using fast quenching coupled with EPR (13) indicates that both iron-sulfur cluster (ISC) and heme b_L are reduced by quinol at the same rate, suggesting a concerted scheme for the bifurcated oxidation of quinol at the Q_P site (13, 14).

Although the concerted mechanism explains why the proposed semiquinone at the Q_P site is not detected (13), the proponents of sequential mechanism argue that similar reduction rates observed in heme b_L and ISC is due to the low (60 μs) time resolution of the instrument used. They attribute the missing semiquinone to its low stability and the fast electron transfer to heme b_L (15). One way to confirm the existence of semiquinone at the Q_P site is using a mutant complex lacking heme b_L. If the sequential mechanism exists, one should expect to see some Q_P site semiquinone in this mutant complex, due to the lack of its electron acceptor, heme b_L.

The first cytochrome bc_1 complex crystallographic structure from bovine heart mitochondria was reported in 1997 (16). Since then, more x-ray crystallographic structures of bc_1 complexes from different species have become available (17–20). Based on the poor electron density of ISP and the larger than expected distance between ISC and heme c_1 in the first crystallographic structure, a need for head domain movement and flexibility of the neck region of ISP were proposed (16–18) and confirmed experimentally (21–27). The head domain of ISP is considered to have two docking positions: *b*-position and c_1-position (17). Reduction of ISP by quinol takes place when the head domain of ISP is located at the *b*-position. It then moves to the c_1-position to reduce cytochrome c_1. Although few investigators question the requirement for movement of the ISP head domain during bc_1 catalysis (17, 21–27), there is no

* This work was supported in part by National Institutes of Health Grant GM30721 (to C. A. Y.). This work was also supported by Oklahoma Agricultural Experiment Station Projects 1819 and 2372 from the Oklahoma State University. The costs of publication of this article were defrayed in part by the payment of page charges. This article must therefore be hereby marked "*advertisement*" in accordance with 18 U.S.C. Section 1734 solely to indicate this fact.

[1] To whom correspondence should be addressed. Tel.: 405-744-6612; Fax: 405-744-6612; E-mail: cayuq@okstate.edu.

[2] The abbreviations used are: ISP, iron-sulfur protein; $Q_0C_{10}BrH_2$, 2,3-dimethoxy-5-methyl-6-(10-bromodecyl)-1,4-benzoquinol; DM, *n*-dodecyl-β-D-maltopyranoside; MCLA, 2-methyl-6-(4-methoxyphenyl)-3,7-dihydroimidazol[1,2-α]pyrazin-3-one, hydrochloride; EPR, electron paramagnetic resonance; ISC, iron-sulfur cluster; ICM, intra-cytoplasmic membrane; P_m, Q_P site inhibitors that enhance the mobility of head domain of iron-sulfur protein; P_f, Q_P site inhibitors that fix the head domain of iron-sulfur protein at *b*-position.

consensus for what the driving force for this movement is (8, 13, 28–31).

One proposed mechanism suggests that movement of reduced ISP head domain from the *b*- to c_1-position is regulated by protein conformational changes induced by electron transfer from heme b_L to heme b_H (13, 31). Recent results (32, 33) of analyses of the binding affinity and inhibitory efficacies of P_m and P_f inhibitors, at different redox states of the cytochrome bc_1 complex, are consistent with this proposal. One way to further substantiate this proposal is to determine the electron transfer activity and pre-steady state reduction rates of hemes c_1, b_L, and b_H, by quinol, in the presence and absence of inhibitors, in mutant complexes lacking heme b_L or heme b_H and compared with those obtained from the wild-type complex. If this proposal is correct, one would expect to see a decrease in electron transfer activity and the rate of heme c_1 reduction in b_H and b_L knock-out mutant complexes.

Formation of superoxide anion is a well established side reaction during the oxidation of quinol by cytochrome bc_1 complex. Addition of antimycin to the intact bc_1 complex increases superoxide production (34–36). The electron leakage (or superoxide production) site can be at the semiquinone (37) of the Q_p site or reduced heme b_L (34, 38), depending on the mechanism by which bifurcation of ubiquinol proceeds. If bifurcation of quinol at the Q_p site proceeds by the sequential mechanism, semiquinone formed at the Q_P site and reduced heme b_L would both be the electron leakage sites during bc_1 catalysis. Thus, one would expect to see at least some increase in superoxide production in the mutant complex lacking heme b_L, due to the possible increase of semiquinone. If bifurcation of ubiquinol at the Q_p site proceeds by the concerted mechanism, reduced heme b_L would be the only electron leakage site, because there will be no semiquinone at the Q_P site during bc_1 catalysis.

The mechanism for superoxide production by the bc_1 complex is unclear. Comparing superoxide production by wild-type and mutant complexes lacking either heme b_L or heme b_H, under various conditions, should provide insight into the superoxide production mechanism.

Herein we report detailed procedures for generating *Rhodobacter sphaeroides* mutants expressing cytochrome bc_1 complex lacking either heme b_L (H198N) or heme b_H (H111N), purifying cytochrome bc_1 complexes from intra-cytoplasmic membranes (ICM) of both mutants, and characterizing the purified mutant complexes in subunit composition, electron transfer activity, absorption spectral properties, redox potential, presteady state reduction kinetics of hemes (b_L, b_H, and c_1), and superoxide production of purified complexes.

EXPERIMENTAL PROCEDURES

Materials—Cytochrome *c* (horse heart, type III), stigmatellin, myxothiazol, antimycin A, and xanthine oxidase were purchased from Sigma. *n*-Dodecyl-β-D-maltopyranoside (DM) and *n*-octyl-β-D-glucopyranoside were from Anatrace. Proteinase K was purchased from Invitrogen. Nickel-nitrilotriacetic acid gel and a Qiaprep spin Miniprep kit were from Qiagen. 2-Methyl-6-(4-methoxyphenyl)-3,7-dihydroimidazol[1,2-α]pyrazin-3-one, hydrochloride (MCLA) was from Molecular Probes, Inc. 2,3-Dimethoxy-5-methyl-6-(10-bromodecyl)-1,4-benzoquinol ($Q_0C_{10}BrH_2$) was prepared as reported previously (39). All other chemicals were of the highest purity commercially available.

TABLE 1
Oligonucleotides used for site-directed mutagenesis
The underlined bases correspond to the genetic codes for the amino acid(s) to be mutated.

	Sequence
H198N(F)[a]	CGGTTCTTCTCGCTGAACTACCTGCTGCCCTTCG
H198N(R)	CGAAGGGCAGCAGGTAGTTCAGCGAGAAGAACCG
H111N(F)	CGCGGTCTATCTGAACATCTTCCGCGGCCTC
H111N(R)	GAGGCCGCGGAAGATGTTCAGATAGACCGCG

[a] F and R in parentheses denote forward and reverse primers, respectively.

Generation of R. sphaeroides Cytochrome bc_1 Mutants—Mutations were constructed by the QuikChange site-directed mutagenesis kit from Stratagene using a supercoiled double-stranded pGEM7Zf(+)-*fbc*B as template. Forward and reverse primers were used for PCR amplification (Table 1). The pGEM7Zf(+)-*fbc*B plasmid (40) was constructed by ligating the NsiI-XbaI fragment from pRKDfbcFBC_{6H}Q into NsiI and XbaI sites of the pGEM7Zf(+) plasmid. The NsiI-XbaI fragment from the pGEM7Zf(+)-*fbc*B_m plasmid was ligated into the NsiI and XbaI sites of the pRKD418-fbcF$B_{Km}C_{6H}$Q plasmid to generate the pRKD418-*fbc*FB_mC_{6H}Q plasmid. A plate-mating procedure (41) was used to mobilize the pRKD418-*fbc*FB_mC_{6H}Q plasmid in *Escherichia coli* S17 cells into *R. sphaeroides* BC17 cells. The presence of engineered mutations was confirmed by DNA sequencing of the NsiI-XbaI fragment as previously reported (41). DNA primers were purchased from Invitrogen. DNA sequencing was performed by the Recombinant DNA/Protein Core Facility at Oklahoma State University.

Enzyme Preparations and Activity Assays—Chromatophores, intracytoplasmic membrane, and the His_6-tagged cytochrome bc_1 complexes were prepared as previously reported (21). To assay cytochrome bc_1 complex activity, chromatophores or purified cytochrome bc_1 complexes were diluted with 50 mM Tris-Cl, pH 8.0, containing 200 mM NaCl and 0.01% DM to a final concentration of cytochrome c_1 of 1 μM. Appropriate amounts of the diluted samples were added to 1 ml of assay mixture containing 100 mM Na^+/K^+ phosphate buffer, pH 7.4, 300 μM EDTA, 100 μM cytochrome *c*, and 25 μM $Q_0C_{10}BrH_2$. Activities were determined by measuring the reduction of cytochrome *c* (the increase of absorbance at 550 nm) in a Shimadzu UV 2401 PC spectrophotometer at 23 °C, using a millimolar extinction coefficient of 18.5 for calculation. The non-enzymatic oxidation of $Q_0C_{10}BrH_2$, determined under the same conditions in the absence of enzyme, was subtracted from the assay.

Determination of Heme Content in bc_1 Complexes—To determine the concentrations of hemes c_1 and *b* in wild-type and mutant complexes of H111N and H198N, purified cytochrome bc_1 samples were diluted to a concentration of 5 μM cytochrome c_1 in 1.0 ml of aqueous solution containing 200 mM NaOH and 40% pyridine. An appropriate amount of $K_3Fe(CN)_6$ was added to assure bc_1 complexes were fully oxidized. Spectra of oxidized bc_1 samples were recorded in a Shimadzu UV-2401 PC spectrophotometer at 23 °C. Solid sodium dithionite (a few

TABLE 2
Difference of millimolar extinction coefficients of reduced pyridine hemochromogen of hemes *b* and c_1 at the selected wavelengths

Hemochromogen	$\epsilon^{549-540\ nm}_{mM}$	$\epsilon^{558-580\ nm}_{mM}$
Heme c_1	21.13	4.28
Heme *b*	9.98	32.86

grains) was then added, and several successive spectra of the reduced pyridine hemochromes were recorded (every 20 s) until there were no significant differences between two consecutive spectra. Table 2 lists the extinction coefficients (42) of pyridine hemochromes used to calculate the concentration of hemes *b* and c_1. To calculate the concentration of hemes *b* and c_1 in a bc_1 sample, the equation pair below was employed. In these equations ϵ stands for the extinction coefficient. The subscript numbers of ϵ indicate the corresponding wavelengths. *C* stands for concentration.

$$C_{c1} \times \epsilon^{c1}_{549-540} + C_b \times \epsilon^{b}_{549-540} = A_{549-540} \quad \text{(Eq. 1)}$$

$$C_{c1} \times \epsilon^{c1}_{558-580} + C_b \times \epsilon^{b}_{558-580} = A_{558-580} \quad \text{(Eq. 2)}$$

Potentiometric Titrations of the Cytochrome b of Mutant Cytochrome bc_1 Complexes—Redox titrations of cytochromes *b* in wild-type and mutant bc_1 complexes were essentially according to the published method (43, 44). 3-ml aliquots of the bc_1 complex (2 μM cytochrome *b*) in 0.1 M Na^+/K^+ phosphate buffer, pH 7.0, containing 25 μM 1,4-benzoquinone (E_m, 293 mV), 2,3,5,6-tetramethyl-*p*-phenylenediamine (E_m, 260 mV), 1,2-naphthoquinone (E_m, 143 mV), phenazine methosulfate (E_m, 80 mV), phenazine ethosulfate (E_m, 55 mV), 1,4-naphthoquinone (E_m, 36 mV), duroquinone (E_m, 5 mV), pyocyanine (E_m, −34 mV), indigo carmine (E_m, −125 mV), and anthraquinone-2-sulfonic acid (E_m, −225 mV) were used. Reductive titrations were carried out by addition of sodium dithionite solution to the ferricyanide-oxidized samples and oxidative titrations by addition of ferricyanide solution to the dithionite-reduced samples. At indicated E_h values during the redox titration, absorption spectra from 600 to 500 nm were taken. The optical absorbance at 560 nm, minus that at 580 nm, was used for determination of cytochrome *b* reduction. Midpoint potentials of cytochrome b_L and b_H were calculated by fitting the redox titration data, using the Nernst equation for a one-electron carrier ($n = 1$), by Kaleidagraph (44).

Fast Kinetics Study—To determine electron transfer rates between the quinol and heme *b* or heme c_1, the cytochrome bc_1 complex was mixed with ubiquinol ($Q_0C_{10}BrH_2$) in equal volume at room temperature in an Applied Photophysics stopped-flow reaction analyzer SX.18MV (Leatherhead, United Kingdom). The concentration of bc_1 complex was 12 μM (based on cytochrome c_1) in 50 mM Tris-Cl, pH 8.0, at 4 °C, containing 200 mM NaCl and 0.01% DM. For use in the stopped-flow, $Q_0C_{10}BrH_2$ in ethanol was diluted to 240 μM in the same buffer. Reductions of cytochrome *b* and cytochrome c_1 in wild-type were monitored by the increase of absorption difference of $A_{560-580}$ and $A_{551-539}$, respectively, with a photodiode array scan between 600 and 500 nm. Reductions of cytochrome b_L in H111N and b_H in H198N were determined from the increase in $A_{565-580}$ and $A_{560-580}$. When an inhibitor was used, the cytochrome bc_1 complex was treated with 5-fold molar excess of inhibitor over heme c_1, for 5 min at 4 °C, prior to the experiment. Because the concentration of ubiquinol used was 20 times higher than that of the cytochrome bc_1 complex, the reactions between bc_1 and quinol were treated as pseudo first-order reactions. Time traces of the reaction were fitted with a first-order rate equation to obtain the pseudo first rate constants k_1 by Kaleidagraph.

Detection of Q Radical at the Q_P Site with EPR—300 μl of 150 μM purified cytochrome bc_1 complexes were treated with 10-fold excess of ubiquinol to fully reduce cytochrome c_1 in 10 s and frozen in liquid nitrogen. EPR spectra were recorded at −170 °C with the following instrument settings: microwave frequency, 9.4 GHz; microwave power, 2.2 milliwatts; modulation amplitudes, 6.3 G; modulation frequency, 100 kHz; time constant, 655.4 ms; sweep time, 167.8 s; conversion time, 163.8 ms.

Determination of Superoxide Production—Superoxide anion generation was determined by measuring the chemiluminescence of the MCLA-$O^{\cdot-}$ adduct (45), in an Applied Photophysics stopped-flow reaction analyzer SX.18MV (Leatherhead, United Kingdom), by leaving the excitation light off and registering light emission (46, 47). Reactions were carried out at 23 °C by mixing 1:1 solutions A and B. Solution A contained 100 mM Na^+/K^+ phosphate buffer, pH 7.4, 1 mM EDTA, 1 mM KCN, 1 mM NaN_3, 0.1% bovine serum albumin, 0.01% DM, and 5.0 μM wild-type or mutant bc_1 complex. Solution B was the same as A with the bc_1 complex being replaced with 125 μM $Q_0C_{10}BrH_2$ and 4 μM MCLA. Once the reaction starts, the produced chemiluminescence in voltage was consecutively monitored for 2 s.

RESULTS AND DISCUSSION

Characterization of Mutants Lacking Either Heme b_L (H198N) or Heme b_H (H111N)—In the cytochrome *b* subunit of cytochrome bc_1 complex from the *R. sphaeroides*, His^{97} and His^{198} are the ligands of heme b_L, whereas His^{111} and His^{212} are the ligands of heme b_H. Two mutants, H198N and H111N, in which histidine 198 and histidine 111 of cytochrome *b* were, respectively, substituted with Asn were constructed and selected for the present study. The H198N mutant knocks out heme b_L, whereas the H111N mutant knocks out heme b_H. Because the cytochrome bc_1 complex is absolutely required for photosynthetic growth of this bacterium, and hemes b_L and b_H constitute the low potential electron transfer chain in the proposed Q-cycle mechanism, it is important to see whether or not these two mutants can support photosynthetic growth. Cultures of wild-type and mutants were placed in a light tank after 4 h of dark grow. Photosynthetic growth was followed by the increase of cell intensity. None of the mutants show any evidence of growth in 6–8 days. To grow cells for the preparation of mutated bc_1 complexes, H198N and H111N were grown semi-aerobically. These two mutants can grow semiaerobically at a rate comparable with that of the wild-type cells. ICM were prepared from semiaerobically grown cells and used for preparation of corresponding mutant complexes.

ICMs prepared from mutants H198N and H111N contain subunits cytochrome *b*, cytochrome c_1, ISP, and subunit IV in the same concentrations as those detected in the wild-type ICM, determined by Western blot using antibodies against

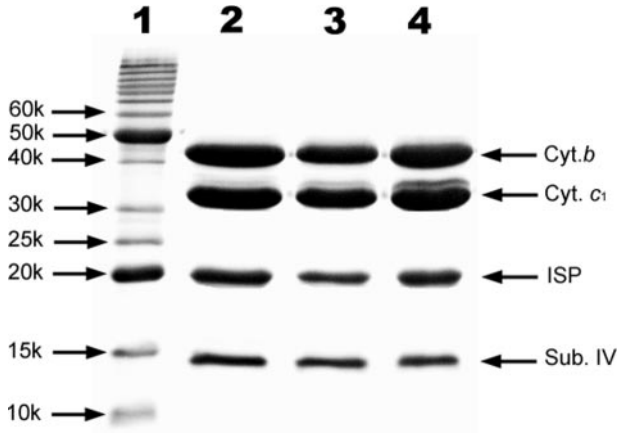

FIGURE 1. **SDS-PAGE of purified cytochrome bc_1 complexes from wild-type and mutants H198N and H111N.** *Lanes 1–4* are for polypeptide standard, wild-type, mutant H198N, and mutant H111N, respectively. Aliquots of purified bc_1 complexes were incubated with 1% SDS and 0.4% β-mercaptoethanol at 37 °C for 20 min. Digested samples containing about 200 pmol of cytochrome c_1 were subjected to electrophoresis. The molecular masses of standard polypeptides are: 10, 15, 20, 25, 30, 40, 50 and 60 kDa.

these four individual proteins. This result indicates that lacking heme b_L in the H198N mutant and lacking heme b_H in the H111N mutant does not impair the complex assembly into the ICM membrane. This finding is contradictory to the previous report (48) that ICMs from mutants lacking heme b_H (H111N, H111D, and H212D) have subunits of cytochromes b and c_1, whereas no such subunits were detected in ICMs from mutants lacking heme b_L (H97N, H97D, H198N, and H198Y). While constructing mutants lacking heme b_L or heme b_H we observed that some heme b_L knocked out mutants, such as H97F and H97N, are unstable, purification attempts were not successful. The structural stability of H198N and H111N mutant complexes in their ICMs enables us to purify and characterize these two mutant complexes with methods similar to those used for the wild-type complex.

Fig. 1 compares SDS-PAGE patterns of purified wild-type and mutant cytochrome bc_1 complexes. The purification procedure involves DM solubilization followed by nickel-affinity gel column chromatography (21). The yields and subunit compositions of purified mutant complexes are comparable with those of the wild-type.

Fig. 2 shows absorption spectra of purified wild-type (A) and mutant complexes of H198N (B) and H111N (C). The presence of cytochromes b_H and b_L in the wild-type complex is revealed by a difference spectrum of dithionite-partially reduced minus ascorbate reduced and a difference spectrum of dithionite-fully reduced minus dithionite-partially reduced, respectively (49). If a catalytic amount of succinate-Q reductase is added to a purified wild-type complex, b_H is observed from a difference spectrum of succinate-reduced minus ascorbate-reduced and b_L from a difference spectrum of dithionite-reduced minus succinate-reduced (50). Ascorbate reduces cytochrome c_1; succinate reduces cytochromes c_1 and b_H; dithionite reduces cytochromes c_1, b_H, and b_L. Cytochrome b_H has an α absorption peak at 560 nm, whereas cytochrome b_L has a double-α peak with absorption at 565 nm and a shoulder at 558 nm (see Fig. 2*A*). The α absorption peak of cytochrome b in the H198N mutant complex (Fig. 2*B*), which is obtained from a difference

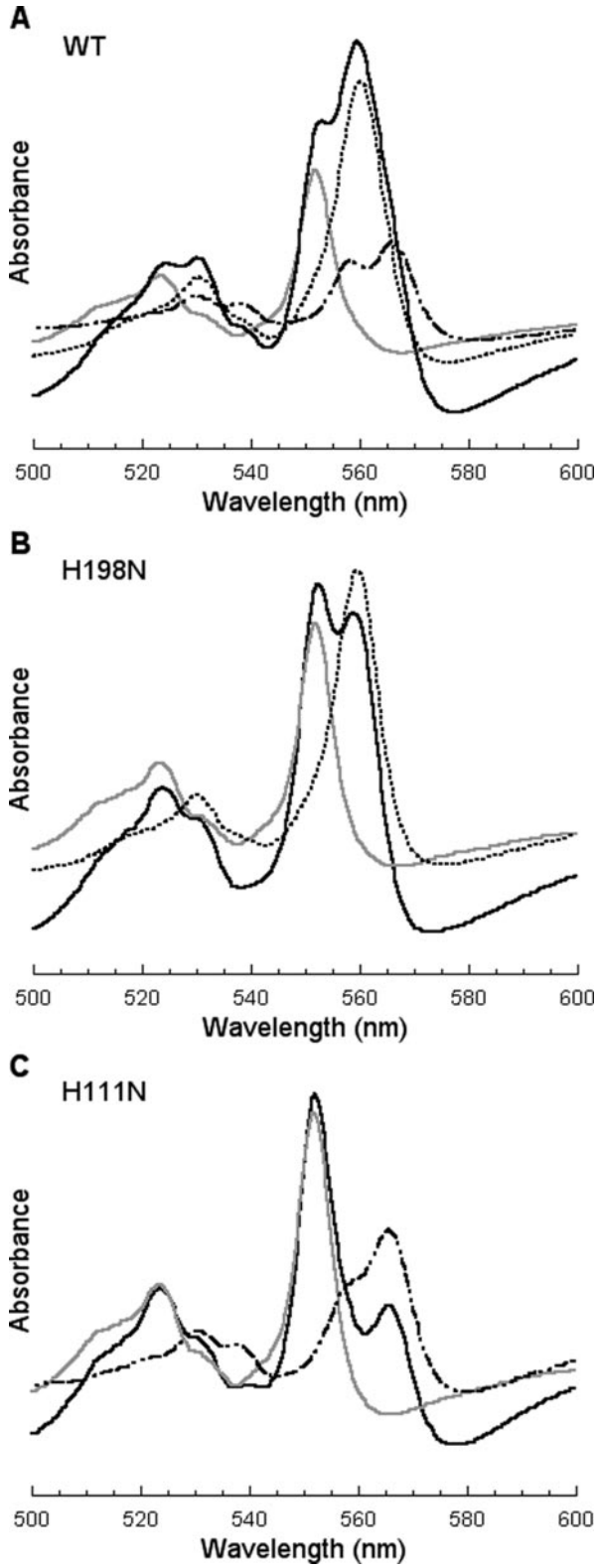

FIGURE 2. **Absorption spectra of wild-type and mutant bc_1 complexes.** *A–C* are for the wild-type (*WT*), mutants H198N and H111N complexes, respectively. The cytochrome c_1 concentration of complexes used was 1 μM for *A*, 1.5 μM for *B* and *C*. The *gray* spectrum stands for ascorbate-reduced sample; and *black solid* spectrum for the dithionite-fully reduced sample. The *black dotted* and *black dot-dash* spectra in *B* and *C*, respectively, are difference spectra of the dithionite-fully reduced minus ascorbate reduced samples. *Black dotted* and *black dot-dash* spectra in *A* are the difference spectra of the dithionite-partially reduced (~−50 mV) minus ascorbate reduced and of the dithionite-fully reduced minus the dithionite-partially reduced, respectively.

TABLE 3
Characterization of mutant H198N and H111N bc_1 complexes

	Wild-type	H198N	H111N
Photosynthetic growth	Yes	No	No
Cytochrome *b*/cytochrome c_1 ratio	1.65	1.0	0.98
Specific activity[a]	3.5	0.4	0.32
Antimycin sensitivity	Yes	36.4%[b]	No
Stigmatellin sensitivity	Yes	Yes	Yes
Myxothiazol sensitivity	Yes	Yes	Yes

[a] The unit of specific activity is μmol of cytochrome *c* reduced/min/nmol of cytochrome c_1.
[b] The 36.4% means the loss of 36.4% of its bc_1 activity upon antimycin treatment.

spectrum of dithionite-reduced minus ascorbate-reduced, is at 560 nm, indicating that only cytochrome b_H is present in this mutant complex. The α peak of cytochrome *b* in the H111N mutant complex is at 565 nm with a shoulder at 558 nm (Fig. 2*C*), indicating that only cytochrome b_L is present in this mutant complex.

To detect the presence of trace amounts of other cytochrome *b* in a given mutant, the complex was titrated with dithionite solution to reduce cytochromes *b* gradually (data not shown). In the mutant H198N complex, the last reduced heme *b* showed a heme b_H absorption spectrum, the same as that of the very first reduced one, suggesting that the H198N mutant complex contains only heme b_H. If there is some heme b_L in this mutant complex, the difference spectrum of the last dithionite reduced minus the second to last dithionite reduced should differ from that of the first dithionite reduced minus ascorbate reduced, because heme b_L is expected to be reduced last due to its low redox potential. In the H111N mutant complex, the difference spectrum of the first dithionite reduced minus ascorbate reduced is the same as the difference spectrum obtained from the last dithionite reduced minus the second to the last dithionite reduced. These two difference absorption spectra are identical to those of heme b_L in the wild-type complex, suggesting that the H111N mutant complex contains only heme b_L.

In general, for bc_1 complexes, hemes *b*, including heme b_L and b_H, are calculated from the difference extinction coefficient of 28.5/mM·cm between 560 and 580 nm in the difference spectrum of dithionite reduced minus ascorbate reduced samples. The heme c_1 is calculated from a difference spectrum of ascorbate reduced minus ferricyanide-oxidized complex using a difference extinction coefficient of 17.5/mM·cm between 551 and 539 nm. Because the extinction coefficient of individual heme b_L and heme b_H is not firmly established, we used the alkaline pyridine hemochromogen spectrum to determine the concentrations of hemes *b* and c_1 in mutant complexes of H198N and H111N. The equations used for calculation are listed under "Experimental Procedures." In the wild-type bc_1 complex the b/c_1 molar ratio is about 1.65. In mutant complexes of H198N and H111N, b/c_1 molar ratios are close to 1.0 (see Table 3). Based on the heme *b* contents determined by pyridine hemochrome and the difference absorption spectra of dithionite reduced minus ascorbate reduced mutant complexes, the difference extinction coefficients for hemes b_L and b_H were calculated to be 12.0/mM·cm between 565 and 580 nm and 24.5/mM·cm between 560 and 580 nm, respectively. The lower than expected b/c_1 ratio in the wild-type complex is probably due to the presence of excess cytochrome c_1 in the complex, as the His tag is located at the C terminus of cytochrome c_1 protein. The presence of excess cytochrome c_1 in the wild-type complex was confirmed by protein crystallization (51, 52). In the crystalline bc_1 complex, the b/c_1 molar ratio is 2. The excess cytochrome c_1 is found in the mother liquid after crystallization.

Effect of Mutations on the Electron Transfer Activity and the Redox Potential of b Hemes—Specific activities of purified mutant complexes were determined and compared with the wild-type complex. Mutant complexes of H198N and H111N have low bc_1 activities, about 9–11% of that in the wild-type complex (Table 3). The bc_1 activity detected in these two mutant complexes is inhibited by stigmatellin and myxothiazol, indicating ubiquinol can bind and be oxidized at the Q_P site in both complexes. As expected, the H111N mutant complex is completely resistant to antimycin. However, it is somewhat surprising that H198N is partially sensitive to antimycin.

To see if these substitutions have any effect on the E_m of heme b_L or heme b_H, E_m values of heme b_L and b_H in mutants H111N and H198N were determined, respectively. As shown in Fig. 3, heme b_H in the H198N mutant complex has an E_m of −35 mV, significantly lower than the E_m of heme b_H in the wild-type complex (50 mV). The E_m of heme b_L in the H111N mutant complex is −95 mV, comparable with that in the wild-type complex (−93 mV). However, this value is lower than that reported by others (48) using ICM of the same mutant. Thus the substitution in mutant H198N has some effect on the E_m of heme b_H, whereas the substitution in mutant H111N has little effect on the E_m of heme b_L. These results seem contradictory to the columbic interaction between hemes b_L and b_H reported in the literature (15, 48).

Effect of Mutations on the Rate of Heme c_1 Reduction by Quinol—The loss of heme b_L and heme b_H in the mutant complexes of H198N and H111N, respectively, provides us an opportunity to study the effect of the low potential chain on c_1 reduction and movement of the ISP head domain. The fast-kinetics study is carried out on the stop-flow instrument of Applied Photophysics Ltd. Fig. 4 shows the time traces of heme c_1 reduction, for 1.2 s, in wild-type and mutant complexes of H198N and H111N. Heme c_1 reduction rates in the two mutant complexes are much lower than that in the wild-type complex. Assuming heme c_1 reduction is a pseudo first-order reaction, the k_1 values are determined to be 11.6, 1.7, and 1.4 s^{-1} for the wild-type and mutant complexes of H198N and H111N, respectively. The heme c_1 reduction rates in the H198N and H111N mutant complexes are only about 15–12% of that in the wild-type complex. Despite of low reduction rates of heme c_1 in the two mutant complexes, maximum levels of heme c_1 reduction are the same as that of the wild-type complex. 50% of the total heme c_1 is reduced by ubiquinol as reported (53). Because the Q_P sites in the H198N and H111 mutant complexes are similar to that in the wild-type complex, as both mutant complexes are sensitive to stigmatellin and myxothiazol (the Q_P site inhibitor), the decrease in rate of heme c_1 reduction is not due to the initial bifurcated oxidation of quinol. Likely, this decrease results from impairment of movement of the head domain of reduced ISP, from the *b*-position to c_1-position,

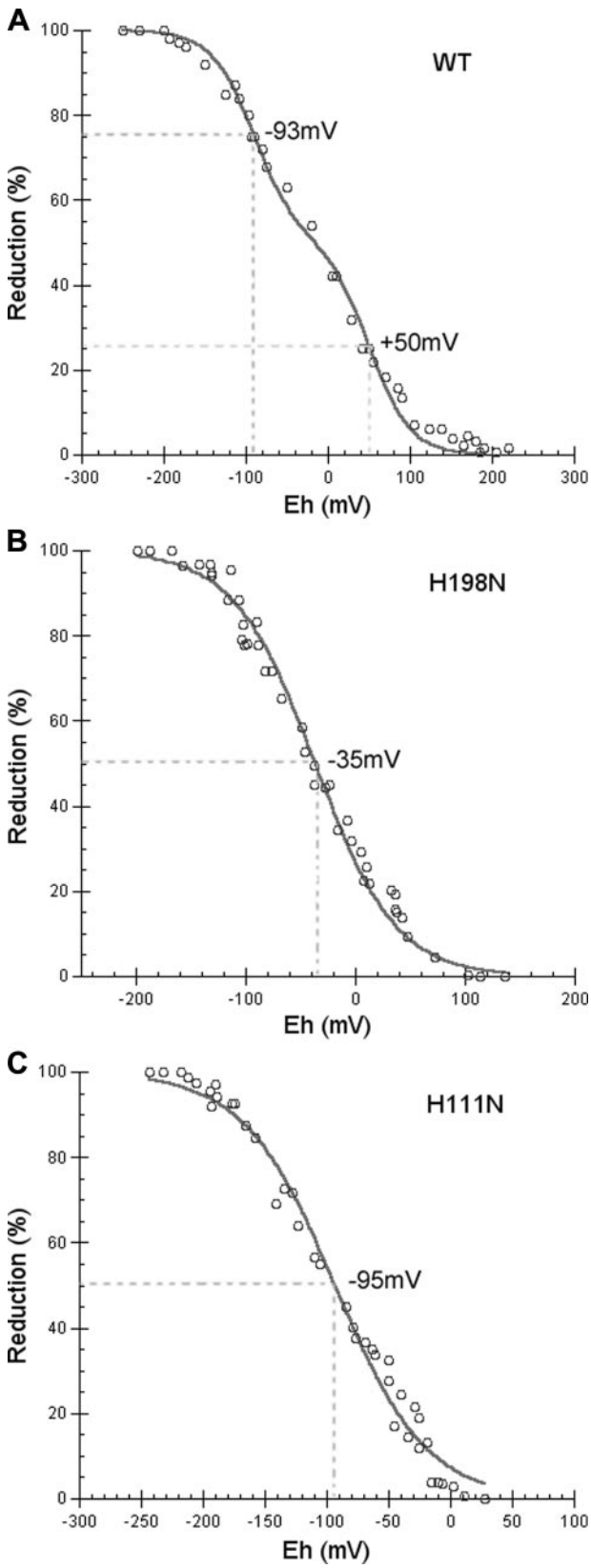

FIGURE 3. **Redox potential titration of heme *b* in wild-type (*A*), H198N (*B*), and H111N (*C*) mutant cytochrome bc_1 complexes.** Oxidative and reductive titrations were performed using potassium ferricyanide and sodium dithionite, respectively, as described under "Experimental Procedures."

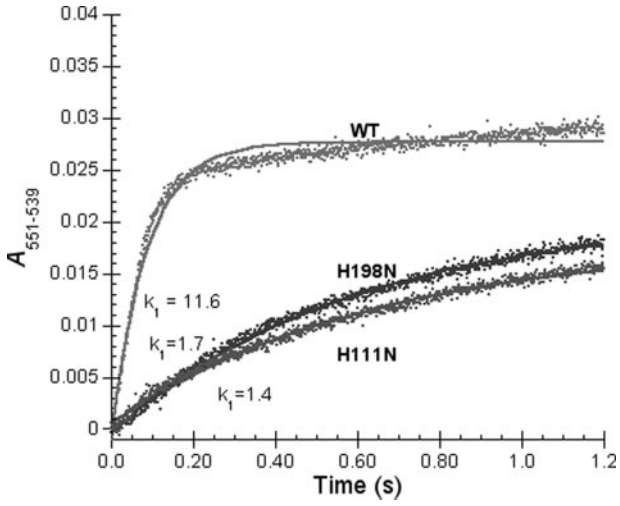

FIGURE 4. **Time trace of heme c_1 reduction by $Q_0C_{10}BrH_2$ in wild-type (*WT*) and mutant complexes.** Experiments were performed with the Applied Photophysics stopped-flow reaction analyzer SX 18MV. Reactions and measurements were performed as described under "Experimental Procedures." The final concentrations of complexes and $Q_0C_{10}BrH_2$ were 6 and 120 μM, respectively. *Solid lines* represent fitted curves.

caused by disruption of electron transfer from heme b_L to heme b_H in these mutant complexes.

Fig. 5 shows the effect of antimycin A and stigmatellin on the reduction rates of heme c_1 in the wild-type and mutant complexes. Antimycin A is a Q_N site inhibitor and stigmatellin is a Q_P site inhibitor. In the wild-type complex antimycin A decreases heme c_1 reduction pseudo first-order rate constant from 11.6 to 4.7 s^{-1} (Fig. 5*A*). This is consistent with the previous report (14) that antimycin A has a significant effect on the reduction rate of heme c_1 in cytochrome bc_1 complexes. In the H198N mutant complex, the rate constant decreases from 1.7 to 1.1 s^{-1}. In the H111N mutant complex, the rate constant decreases from 1.4 to 1.0 s^{-1}. Because both mutant complexes, in which no intact low potential chain is available, also show a decreased rate of heme c_1 reduction in the presence of antimycin A, similar to that observed in the wild-type complex, this inhibitor effect cannot be due to blocking of electron transfer in the low potential chain. It is probably due to the long range effect of antimycin on the Q_P site binding to the Q_N site. In other words, the effect of antimycin A on the heme c_1 reduction rate is not through the low potential redox component but through the cytochrome *b* protein subunit.

Addition of stigmatellin to the wild-type and mutant complexes abolishes heme c_1 reduction. These results further confirm that the Q_P site in these two mutant complexes is functional.

Effect of Mutations on the Rates of Heme b_L and Heme b_H Reductions by Quinol—Fig. 6 shows hemes *b* reduction by quinol, in the presence and absence of antimycin and stigmatellin, in wild-type and mutant bc_1 complexes. In the H198N mutant complex (Fig. 6*B*), a small portion of heme b_H is reduced by quinol, in the absence of inhibitors, and the reduction is biphasic. The rate constants for the fast and slow reduction phases are 12.4 and 0.86 s^{-1}, respectively. Fast phase reduction is abolished when antimycin is present. As

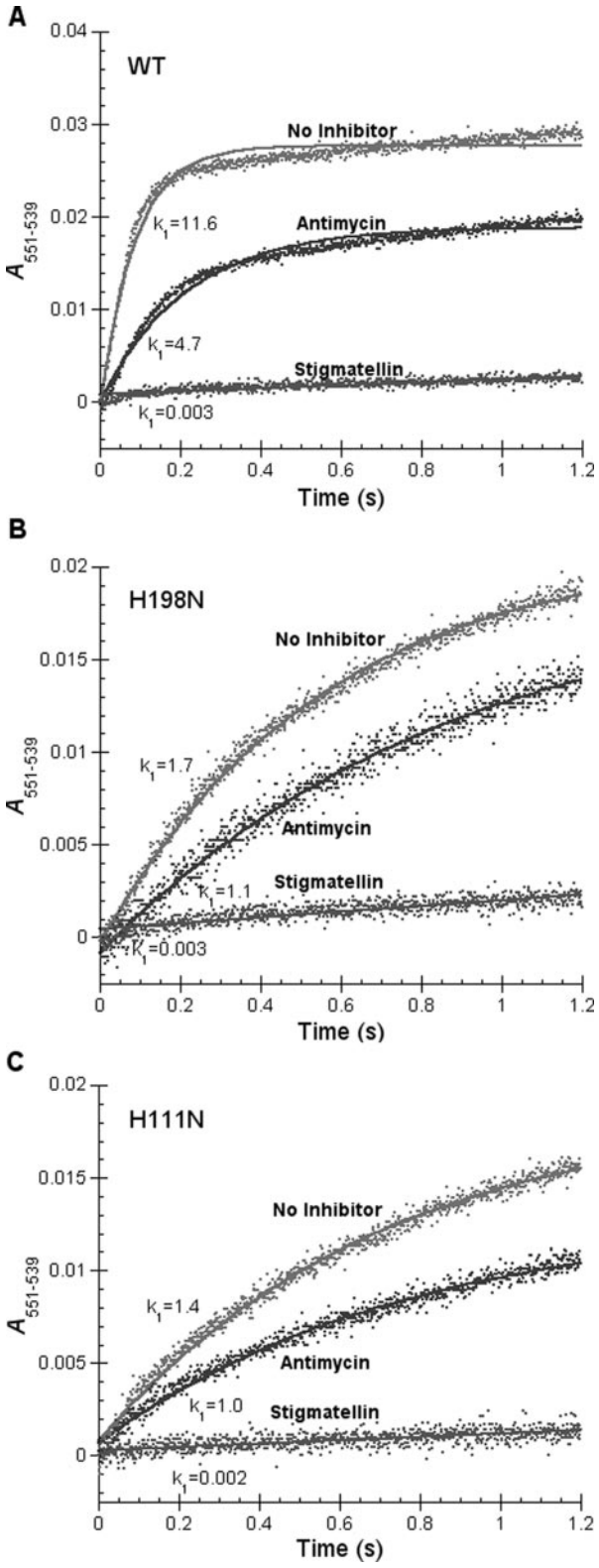

FIGURE 5. **Time trace of cytochrome c_1 reduction by $Q_0C_{10}BrH_2$ in the wild-type (*A*) and mutants H198N (*B*) and H111N (*C*) complexes in the presence of inhibitors.** Experimental conditions were the same as that in Fig. 4 except for the presence of inhibitors. *Solid lines* represent fitted curves.

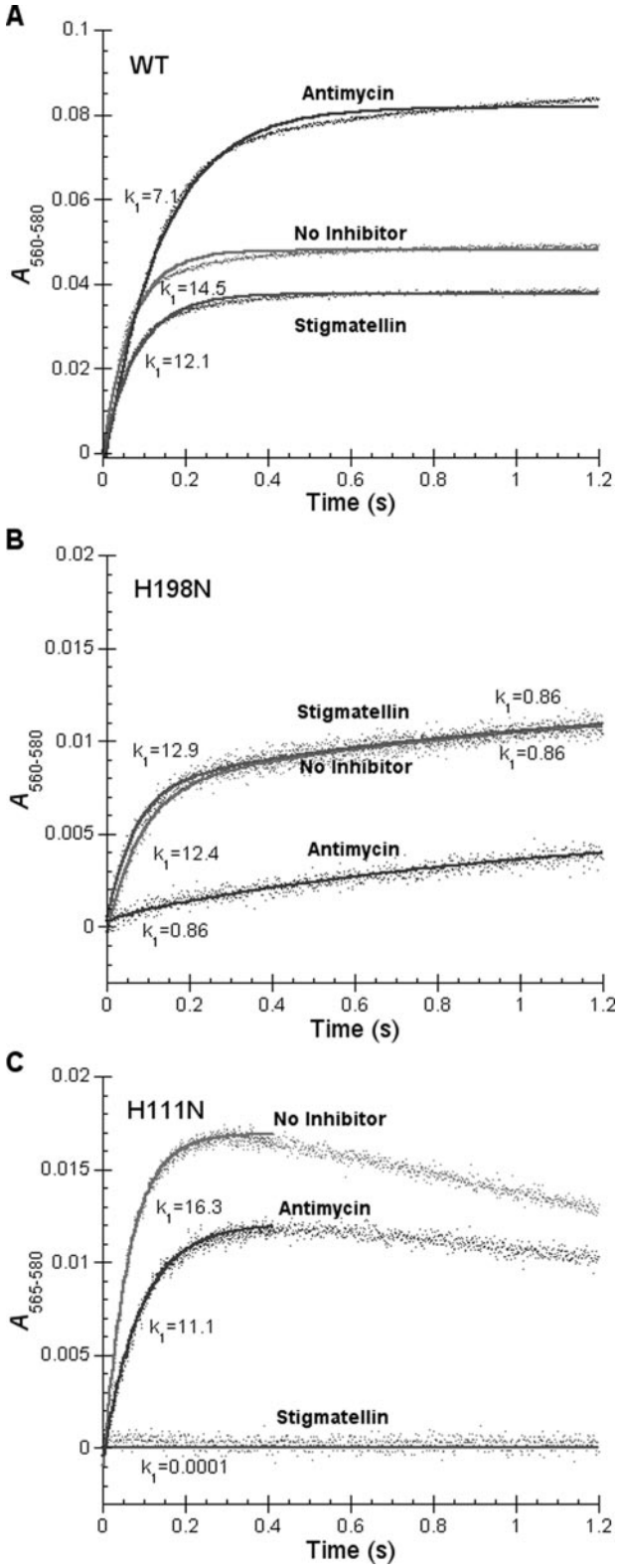

FIGURE 6. **Time trace of cytochrome *b* reduction by $Q_0C_{10}BrH_2$ in wild-type (*A*) and H198N (*B*) and H111N (*C*) mutant complexes.** Reactions and measurements were performed as described under "Experimental Procedures." The reaction was monitored by photodiode array scanning for 1.26 s. Reductions of cytochromes b_L and b_H, were determined from the increase in $A_{565-580}$ and $A_{560-580}$. Cytochrome *b* (including b_L and b_H) was determined from the increase in $A_{560-580}$.

expected, the presence of stigmatellin has little effect because heme b_H is reduced by quinol through the Q_N site, not the Q_P site.

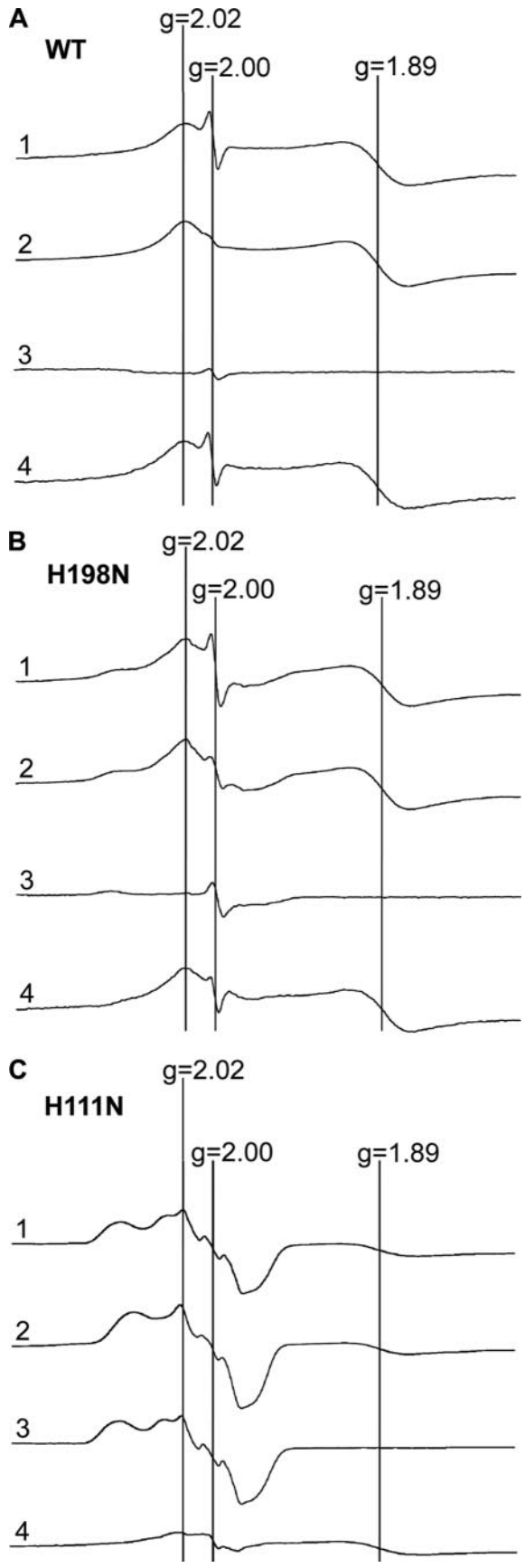

FIGURE 7. **EPR spectra of ISP and free radical (semiquinone) under different conditions.** Purified wild-type (*WT*) (*A*), H198N (*B*), and H111N (*C*) bc_1 complexes were treated with 10-fold excess of $Q_0C_{10}BrH_2$ solution, to fully reduce cytochrome c_1, and frozen in liquid nitrogen. EPR spectra were recorded at −170 °C with the following instrument settings: microwave frequency, 9.4 GHz; microwave power, 2.2 milliwatts; modulation amplitudes, 6.3 G; modulation frequency, 100 kHz; time constant, 655.4 ms; sweep time, 167.8 s; conversion time, 163.8 ms. *Curve 1* is the spectrum for cytochrome bc_1 complexes reduced by $Q_0C_{10}BrH_2$; *curve 2* for those reduced by $Q_0C_{10}BrH_2$ in the presence of antimycin; *curve 3* for ferricyanide-oxidized cytochrome bc_1 complexes; *curve 4* for the spectrum derived from *curve 1* minus *curve 2*. The absence of signals of reduced ISP defines the fully oxidized state of the complex. For mutant H111N, the signal intensities were reduced to one-third to fit in the figure.

In the H111N mutant complex (Fig. 6*C*), a small portion of heme b_L is rapidly reduced by quinol, in the absence of inhibitors, with a reduction rate constant of about 16.3 s^{-1}, followed by a slow reoxidation. It is likely that the reoxidation of heme b_L will lead to superoxide formation. The slower decay rate of superoxide formed in the H111N complex as compared with that formed in the H198N complex, as will be described in Fig. 8, *B* and *C*, supports this speculation. Addition of stigmatellin abolishes this reduction. Addition of antimycin affects the rate and extent of heme b_L reduction: the rate constant decreases from 16.3 to 11.1 s^{-1} and the extent of b_L reduction decreases by 30%. In the wild-type complex antimycin also affects both the rate and extent of heme *b* reduction by quinol (see Fig. 6*A*): it decreases the rate but increases the extent (14, 54–58). It should be noted that heme *b* reduction observed in the wild-type complex, in the absence of inhibitor, is mostly heme b_H. The input of electron for reduction could come from the Q_P site via heme b_L, and less likely, directly from quinol at the Q_N site, because the reduction rate of heme b_L ($k_1 = 16.3\ s^{-1}$) is larger than that of heme b_H ($k_1 = 12.4\ s^{-1}$) (Fig. 6, *B* and *C*). These results seem contradictory to a report indicating that the rate of heme b_H reduction is larger than that of heme b_L in the yeast cytochrome bc_1 complex (59). The observation that the reduction rate of heme b_L in the H111N mutant complex is similar to, albeit higher than, that of the wild-type complex (see Fig. 6*A*) indicates that the Q_P site in this mutant complex is functional. This finding further supports the idea that antimycin has a long range effect on the Q_P site to decrease the rates of heme c_1 and heme b_L reduction.

Attempt to Detect Q Radical at the Q_P Site with Mutant H198N—Because H198N has no heme b_L, and thus no electron acceptor for semiquinone, more semiquinone radical would have increased if the sequential mechanism for bifurcated quinol oxidation is functioning. Fig. 7 shows EPR spectra from wild-type and mutant bc_1 complexes. In the absence of antimycin a strong signal at $g = 2.00$ is observed in the quinol-reduced cytochrome bc_1 complexes from wild-type (Fig. 7*A*, *curve 1*) and mutant H198N (Fig. 7*B*, *curve 1*). This signal decreases significantly when antimycin is added (Fig. 7, *A* and *B*, *curve 2*). Apparently the portion of signal that disappears (Fig. 7, *A* and *B*, *curve 4*) is the signal of semiquinone radical at the Q_N site. However, the signal portion that is insensitive to antimycin is not the long missing semiquinone at the Q_P site, because it is also present in fully oxidized complexes of wild-type and mutant H198N (Fig. 7, *A* and *B*, *curve 3*). It should be noted that this free radical, of unknown origin, is much more concentrated in the H198N complex than in the wild-type complex. Its origin is currently under investigation.

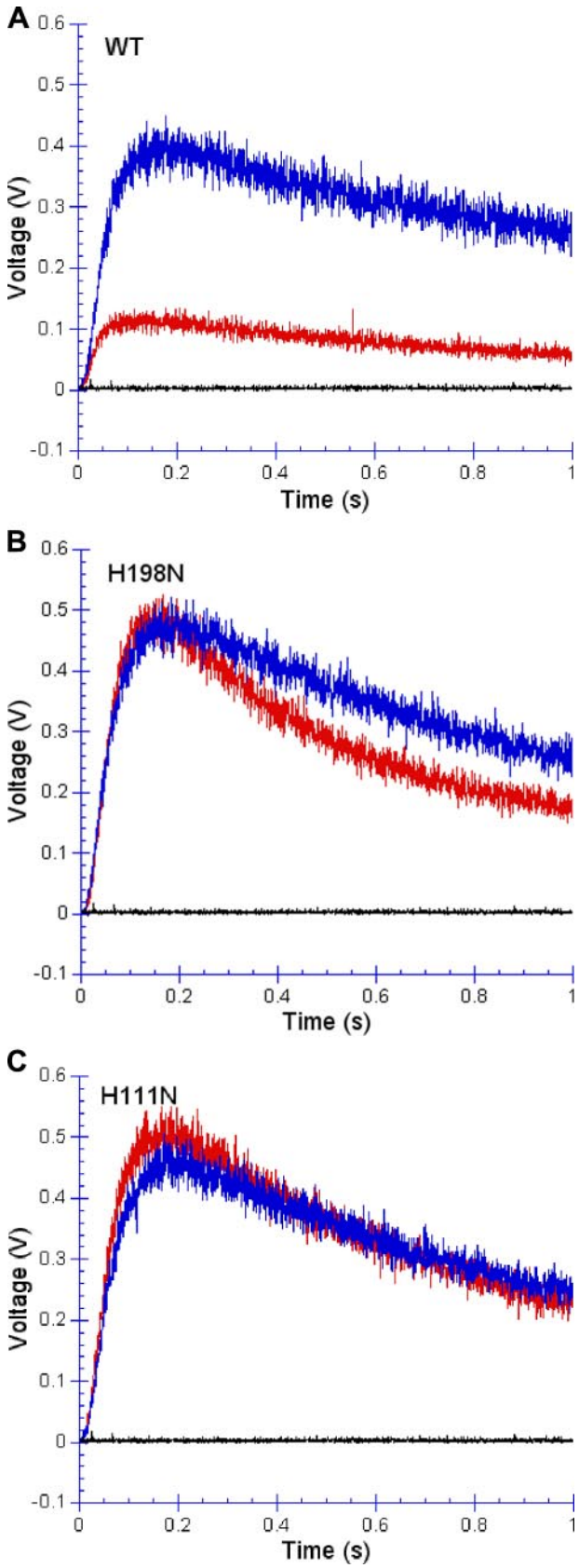

FIGURE 8. **Superoxide production of wild-type and mutant H198N and H111N cytochrome bc_1 complexes.** Superoxide production was measured as described under "Experimental Procedures." *Red* tracings represent complexes without any treatment. *Blue* and *black* tracings are for complexes with antimycin, and ascorbate treatment, respectively.

The EPR spectra for mutant H111N bc_1 complex (Fig. 7*C*) were also determined. Oxidized H111N has an unusual EPR spectrum that is not due to contamination. This spectrum appears to be a characteristic of mutants lacking heme b_H, because another heme b_H-deficient mutant, H212N, has a similar EPR spectrum (data not shown). The concentrations of ISP in all three complexes were about the same, as indicated by the $g = 1.89$ signal. The $g = 1.89$ signal in Fig. 7*C* looks smaller because the intensity of the spectrum was reduced to one-third of the original to compare the signals in the $g = 2.00$ region, of the three complexes.

Superoxide Production in Mutant bc_1 Complexes during Catalysis—Because there is no heme b_L in the H198N and no heme b_H in the H111N, it should be easier for oxygen to get electrons, from either semiquinone or the reduced heme b_L, in these mutant complexes than in the wild-type. Fig. 8 shows superoxide production by mutant and wild-type complexes under different conditions. In the absence of antimycin (*red* tracings), production of superoxide anion by mutant complexes of H198N (Fig. 8*B*) and H111N (Fig. 8*C*) is much greater than by the wild-type (Fig. 8*A*). At the point of strongest chemiluminescence output, superoxide production by H198N and H111N is about 5 times that of the wild-type complex. Antimycin significantly increases superoxide production but slightly decreases its production rate in the wild-type complex (blue tracing in Fig. 8*A*). Antimycin has little effect on the superoxide production in mutants H198N and H111N (*blue tracings* in Fig. 8, *B* and *C*). This lack of effect of antimycin on superoxide production by H198N and H111N indicates that superoxide is produced at the Q_P site, not at the Q_N site. Thus during bc_1 catalysis, oxygen can only get electrons from reduced heme b_L or from semiquione at the Q_P site.

In bc_1 complexes with fully reduced ISP and cytochrome c_1, no chemiluminescence ($O_2^{\cdot-}$) is observed upon the addition of quinol (*black tracings* in Fig. 8), indicating that superoxide production is dependent on ISP reduction by quinol. Therefore, quinol at the Q_P site transfers its first electron to ISC; the second electron, either transferred to heme b_L or retained as semiquinone, reacts with oxygen to produce superoxide. Because there is no detectable semiquinone radical at the Q_P site, molecular oxygen may share quinol electrons with ISP when heme b_L is not available. Normally reduced heme b_L may leak its electron to oxygen. This leakage increases when the low potential electron transfer chain is blocked by antimycin. Because reduction of ISC is the first reaction in both superoxide generation and cytochrome *c* reduction catalyzed by bc_1 complex, the similar activation energy (60) for these reactions seems reasonable, if the reduction of ISC is rate-limiting.

Acknowledgment—We thank Dr. Roger Koeppe for critical review of this manuscript.

REFERENCES

1. Trumpower, B. L., and Gennis, R. B. (1994) *Annu. Rev. Biochem.* **63,** 675–716
2. Erecinska, M., Chance, B., Wilson, D. F., and Dutton, P. L. (1972) *Proc. Natl. Acad. Sci. U. S. A.* **69,** 50–54
3. Wikstrom, M. K. F., and Berden, J. A. (1972) *Biochim. Biophys. Acta* **283,**

403–420
4. Alexandre, A., and Lehninger, A. L. (1979) *J. Biol. Chem.* **254,** 11555–11560
5. Mitchell, P. (1976) *J. Theor. Biol.* **62,** 327–367
6. Brandt, U., and Trumpower, B. (1994) *Crit. Rev. Biochem. Mol. Biol.* **29,** 165–197
7. Crofts, A. R. (2004) *Annu. Rev. Physiol.* **66,** 689–733
8. Link, T. A. (1997) *FEBS Lett.* **412,** 257
9. Junemann, S., Heathcote, P., and Rich, P. R. (1998) *J. Biol. Chem.* **273,** 21603–21607
10. Zhang, H., Osyczka, A., Dutton, P. L., and Moser, C. C. (2007) *Biochim. Biophys. Acta* **1767,** 883–887
11. De Vries, S., Albracht, S. P., Berden, J. A., and Slater, E. C. (1981) *J. Biol. Chem.* **256,** 11996–11998
12. Cape, J. L., Bowman, M. K., and Kramer, D. M. (2007) *Proc. Natl. Acad. Sci. U. S. A.* **104,** 7887–7892
13. Zhu, J., Egawa, T., Yeh, S.-R., Yu, L., and Yu, C.-A. (2007) *Proc. Natl. Acad. Sci. U. S. A.* **104,** 4864–4869
14. Snyder, C. H., Gutierrez-Cirlos, E. B., and Trumpower, B. L. (2000) *J. Biol. Chem.* **275,** 13535–13541
15. Crofts, A. R., Holland, J. T., Victoria, D., Kolling, D. R. J., Dikanov, S. A., Gilbreth, R., Lhee, S., Kuras, R., and Kuras, M. G. (2008) *Biochim. Biophys. Acta* **1777,** 1001–1019
16. Xia, D., Yu, C.-A., Kim, H., Xia, J.-Z., Kachurin, A. M., Zhang, L., Yu, L., and Deisenhofer, J. (1997) *Science* **277,** 60–66
17. Zhang, Z., Huang, L., Shulmeister, V. M., Chi, Y.-I., Kim, K. K., Hung, L.-W., Crofts, A. R., Berry, E. A., and Kim, S.-H. (1998) *Nature* **392,** 677–684
18. Iwata, S., Lee, J. W., Okada, K., Lee, J. K., Iwata, M., Rasmussen, B., Link, T. A., Ramaswamy, S., and Jap, B. K. (1998) *Science* **281,** 64–71
19. Hunte, C. (2001) *FEBS Lett.* **504,** 126–132
20. Lange, C., and Hunte, C. (2002) *Proc. Natl. Acad. Sci. U. S. A.* **99,** 2800–2805
21. Tian, H., Yu, L., Mather, M. W., and Yu, C.-A. (1998) *J. Biol. Chem.* **273,** 27953–27959
22. Kim, H., Xia, D., Yu, C.-A., Xia, J.-Z., Kachurin, A. M., Zhang, L., Yu, L., and Deisenhofer, J. (1998) *Proc. Natl. Acad. Sci. U. S. A.* **95,** 8026–8033
23. Tian, H., White, S., Yu, L., and Yu, C.-A. (1999) *J. Biol. Chem.* **274,** 7146–7152
24. Xiao, K., Yu, L., and Yu, C.-A. (2000) *J. Biol. Chem.* **275,** 38597–38604
25. Darrouzet, E., Valkova-Valchanova, M., and Daldal, F. (2000) *Biochemistry* **39,** 15475–15483
26. Darrouzet, E., Valkova-Valchanova, M., Moser, C. C., Dutton, P. L., and Daldal, F. (2000) *Proc. Natl. Acad. Sci. U. S. A.* **97,** 4567–4572
27. Darrouzet, E., and Daldal, F. (2002) *J. Biol. Chem.* **277,** 3471–3476
28. Brandt, U., and von Jagow, G. (1991) *Eur. J. Biochem.* **195,** 163–170
29. Crofts, A. R., Hong, S., Zhang, Z., and Berry, E. A. (1999) *Biochemistry* **38,** 15827–15839
30. Xia, D., Esser, L., Yu, L., and Yu, C.-A. (2007) *Photosynth. Res.* **92,** 17–34
31. Brandt, U., Haase, U., Schagger, H., and von Jagow, G. (1991) *J. Biol. Chem.* **266,** 19958–19964
32. Cen, X., Yu, L., and Yu, C.-A. (2008) *FEBS Lett.* **582,** 523–526
33. Yu, C.-A., Cen, X., Ma, H.-W., Yin, Y., Yu, L., Esser, L., and Xia, D. (2008) *Biochim. Biophys. Acta* **1777,** 1038–1043
34. Muller, F., Crofts, A. R., and Kramer, D. M. (2002) *Biochemistry* **41,** 7866–7874
35. Zhang, L., Yu, L., and Yu, C.-A. (1998) *J. Biol. Chem.* **273,** 33972–33976
36. Sun, J., and Trumpower, B. L. (2003) *Arch. Biochem. Biophys.* **419,** 198–206
37. Turrens, J. F., Alexandre, A., and Lehninger, A. L. (1985) *Arch. Biochem. Biophys.* **237,** 408–414
38. Nohl, H., and Jordan, W. (1986) *Biochem. Biophys. Res. Commun.* **138,** 533–539
39. Yu, C. A., and Yu, L. (1982) *Biochemistry* **21,** 4096–4101
40. Xiao, K., Liu, X., Yu, C.-A., and Yu, L. (2004) *Biochemistry* **43,** 1488–1495
41. Mather, M. W., Yu, L., and Yu, C.-A. (1995) *J. Biol. Chem.* **270,** 28668–28675
42. Berry, E. A., and Trumpower, B. L. (1987) *Anal. Biochem.* **161,** 1–15
43. Dutton, P. L. (1978) *Methods Enzymol.* **54,** 411–435
44. Liu, X., Yu, C.-A., and Yu, L. (2004) *J. Biol. Chem.* **279,** 47363–47371
45. Nakano, M. (1990) *Methods Enzymol.* **186,** 585–591
46. Denicola, A., Souza, J., Gatti, R. M., Augusto, O., and Radi, R. (1995) *Free Radic. Biol. Med.* **19,** 11–19
47. Gong, X., Yu, L., Xia, D., and Yu, C.-A. (2005) *J. Biol. Chem.* **280,** 9251–9257
48. Yun, C. H., Crofts, A. R., and Gennis, R. B. (1991) *Biochemistry* **30,** 6747–6754
49. Yu, L., Mei, Q. C., and Yu, C. A. (1984) *J. Biol. Chem.* **259,** 5752–5760
50. Yu, C.-A., and Yu, L. (1980) *Biochim. Biophys. Acta* **591,** 409–420
51. Elberry, M., Xiao, K., Esser, L., Xia, D., Yu, L., and Yu, C.-A. (2006) *Biochim. Biophys. Acta* **1757,** 835–840
52. Esser, L., Elberry, M., Zhou, F., Yu, C.-A., Yu, L., and Xia, D. (2008) *J. Biol. Chem.* **283,** 2846–2857
53. Covian, R., Gutierrez-Cirlos, E. B., and Trumpower, B. L. (2004) *J. Biol. Chem.* **279,** 15040–15049
54. King, T. E., Yu, C. A., Yu, L., and Chiang, Y. L. (1975) in *Electron Transfer Chains and Oxidative Phosphorylation* (Van Dam, K., and Van Gelder, B. F., eds) pp. 105–118, North-Holland Publishing Co., Amsterdam, Oxford, American Elsevier Publishing Co., Inc., New York
55. De Vries, S., Albracht, S. P. J., Berden, J. A., and Slater, E. C. (1982) *Biochim. Biophys. Acta* **681,** 41–53
56. De Vries, S., Albracht, S. P. J., Berden, J. A., Marres, C. A. M., and Slater, E. C. (1983) *Biochim. Biophys. Acta* **723,** 91–103
57. Snyder, C. H., and Trumpower, B. L. (1999) *J. Biol. Chem.* **274,** 31209–31216
58. Crofts, A. R., Shinkarev, V. P., Kolling, D. R. J., and Hong, S. (2003) *J. Biol. Chem.* **278,** 36191–36201
59. Rotsaert, F. A. J., Ding, M. G., and Trumpower, B. L. (2008) *Biochim. Biophys. Acta* **1777,** 211–219
60. Forquer, I., Covian, R., Bowman, M. K., Trumpower, B. L., and Kramer, D. M. (2006) *J. Biol. Chem.* **281,** 38459–38465